Pseudodata Analysis of Acceptance Averaging

Internal Report to the JLab E91-011 Collaboration

J. J. Kelly[1] and O. Gayou[2]

[1]*Department of Physics, University of Maryland, College Park, Maryland 20742, USA*
[2]*Department of Physics, Massachusetts Institute of Technology, Cambridge, Massachusetts 02139, USA*

(Dated: December 13, 2004; revised August 5, 2005)

The effects of acceptance averaging upon extraction of recoil polarizations and response functions for the $p(\vec{e}, e'\vec{p})\pi^0$ reaction near the Δ resonance are studied using pseudodata. The kinematical distributions were taken from real data but polarizations at the target were calculated from a reaction model and transported to the focal-plane polarimeter (FPP) using the same spectrometer model employed for data analysis. The azimuthal scattering angle was then sampled randomly based upon the FPP analyzing power. Both polarization and response functions were extracted using the maximum-likelihood method and compared with model input. We find that the response function data are faithful to the input model provided that suitable corrections are made for acceptance averaging, mainly the variation of acceptance-averaged Q^2 with $x = \cos\theta_\pi$. However, serious systematic errors are sometimes encountered for polarization data binned with respect to (W, Q^2, x, ϕ). These errors are caused by magnification of kinematical variations by the lab to cm transformation and cannot be corrected after binning. Eventwise application of kinematic and geometrical factors in the response-function analysis minimizes the sensitivity of those data to acceptance averaging.

I. INTRODUCTION

This report presents the results of a pseudodata analysis performed using the new `PALM++` code. The purpose of this exercise was to: 1) test the internal consistency of the code; 2) evaluate the effects of acceptance averaging; and 3) obtain new insight into persistent problems in the real polarization data. We satisfied ourselves of the internal consistency of the code using many careful but undocumented tests. Here we concentrate on acceptance averaging and consistency among several methods of extracting data. Our conclusions will guide the final analysis of the real data.

Pseudodata were generated for the central bin with $W = 1.232 \pm 0.02$ GeV and $Q^2 = 1.0 \pm 0.2$ (GeV/c)^2. The angular binning remains the same as used in Rikki's thesis. Pseudodata were constructed by the following procedure. Events were read from data files. The reconstructed kinematics were used to compute cross sections, polarizations, and response functions based upon the MAID2000 model. The polarizations were transported to the focal plane using the full spin transformation matrix. The observed polar scattering angle was retained but the azimuthal angle was sampled randomly, using a rejection algorithm, based upon the parametrized analyzing power and the model polarization at the focal plane. The pseudodata were then analyzed using our maximum-likelihood method with one iteration. This procedure produces both polarizations binned in (W, Q^2, x, ϕ) and response functions binned in (W, Q^2, x). Ideally both sets of data should be consistent because the weights for the response analysis are derived from those for the polarization analysis, with additional factors that extract the known ϕ dependencies of polarization components. In addition, reduced response functions were obtained by including the leading $\sin\theta_{cm}$ dependencies in the likelihood weights. It was expected that eventwise inclusion of all known angular factors would reduce the effects of acceptance averaging, such that extracted values for reduced response functions would be close to those for acceptance-averaged kinematics.

In Sec. II we compare two methods for adjusting response functions for variations of acceptance-averaged (W, Q^2) with polar angle. Section II B evaluates the sensitivity of polarization data to differences between central and average ϕ. The consistency between response function and polarization data is studied in Sec. III. A discussion of the sensitivity of binned polarization data to acceptance averaging is given in Sec. IV. Finally, our conclusions are summarized in Sec. V.

II. METHODS FOR BIN CENTERING

Multipole amplitudes are functions of (W, Q^2), but the acceptance averaged $(\overline{W}, \overline{Q^2})$ depend upon $x = \cos\theta_\pi^{(cm)}$. Consequently, Legendre coefficients or multipole amplitudes fitted to angular distributions can be distorted by the x variations of $(\overline{W}, \overline{Q^2})$. Two methods for compensating for such distortions have been implemented in `EPIPROD` and will be tested here using `PALM` pseudodata. In Sec. II A we test those methods using pseudodata for response functions and in Sec. II B we evaluate the sensitivity of polarization calculations to acceptance averaging of ϕ.

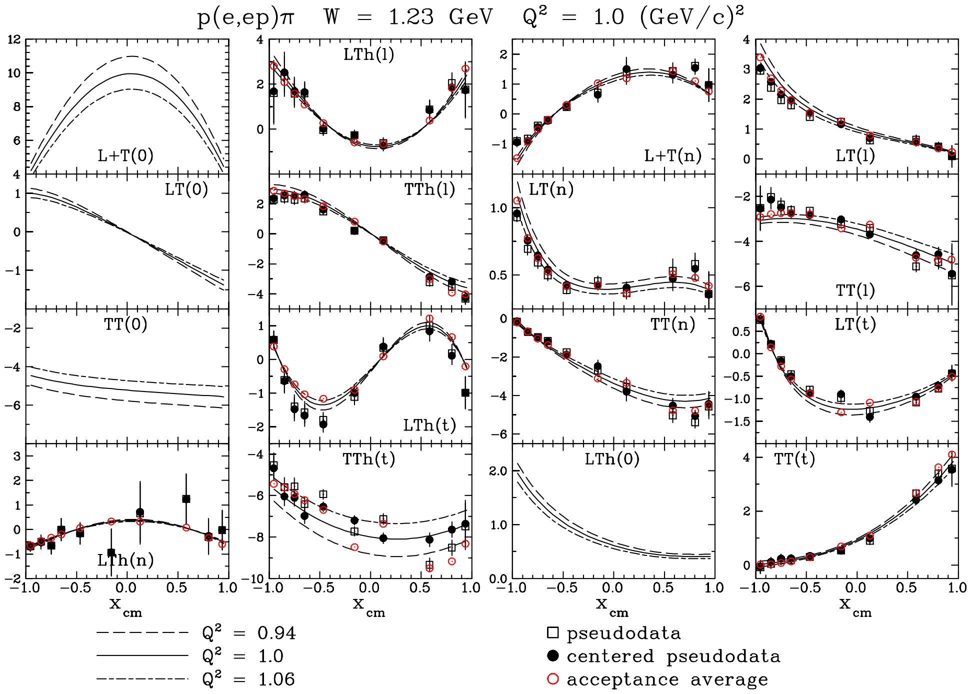

FIG. 1: Pseudodata data for response functions at $W = 1.23 \pm 0.01$ GeV and $Q^2 = 1.0 \pm 0.2$ (GeV/c)^2 are compared with the input model (MAID2000) at the central kinematics and neighboring values of Q^2 representative of the x dependence of acceptance averaging. Acceptance-averaged calculations are shown as red open circles and pseudodata as open squares. Filled circles show pseudodata with additive kinematical corrections based upon MAID2000.

A. Pseudodata tests of additive versus multiplicative algorithms

The additive method is based upon the first-order expansion

$$R(W, Q^2, \bar{x}, \bar{\epsilon}) = R(\overline{W}, \overline{Q^2}, \bar{x}, \bar{\epsilon}) - \frac{\partial R}{\partial W}(\overline{W} - W) - \frac{\partial R}{\partial Q^2}(\overline{Q^2} - Q^2) \tag{1}$$

where overlines indicate acceptance averaging and where the derivatives are evaluated at central kinematics using a model, such as MAID. The primary effect is to compensate for the x dependence of $\overline{Q^2}$ which, though small, reduces systematic irregularities in the data. This procedure is illustrated in Fig. 1 using pseudodata for reduced response functions. Data for unpolarized response functions and R'_{LT} are omitted because the cross section data were projected to central kinematics by Z. Chai using a related procedure. The open squares show raw response functions extracted from pseudodata while open red circles show acceptanced-averaged response functions from MAID2000. The agreement between these data sets, modulo statistical fluctuations, demonstrates the internal consistency of the simulation/analysis program. However, the x dependence of $\overline{Q^2}$ can produce significant systematic deviations from the input model (solid curves) evaluated at central kinematics, especially for R'^{t}_{TT}. Recognizing that $\overline{Q^2} \approx 0.94$ for $x > 0.5$ or 1.06 (GeV/c)^2 for $x < -0.5$, we observe that the pseudodata for R'^{t}_{TT} do cluster around the model curve for the appropriate Q^2. Even the abrupt transition across $x = 0$ is reproduced. The solid circles show that "centered" pseudodata adjusted according to Eq. (1) cluster better around the model curves for central kinematics. Therefore, distortion of multipole amplitudes by the x dependence of $\overline{Q^2}$ should be minimized by fitting centered data.

Additive kinematical corrections have the advantage that variations of both W and Q^2 can be accommodated, but this procedure has the disadvantage that it relies upon a model and we have no model that provides a uniformly good fit to all of the response functions. While that is not a problem for pseudodata, the use of an inaccurate model to make kinematical corrections to real data could introduce more serious errors than it corrects. Therefore, a second procedure based upon form factors was tested. Assuming that all response functions share a common form factor, and that kinematical corrections are dominated by the x-dependence of $\overline{Q^2}$, we postulate

$$R(W, Q^2, \bar{x}) = R(\overline{W}, \overline{Q^2}, \bar{x}) \left(G(Q^2)/G(\overline{Q^2}) \right)^2 \tag{2}$$

and approximate $G(Q^2)$ by the usual dipole form factor $G_D(Q^2) = (1 + Q^2/\Lambda^2)^{-2}$ where $\Lambda^2 = 0.71$ (GeV/c)^2. This

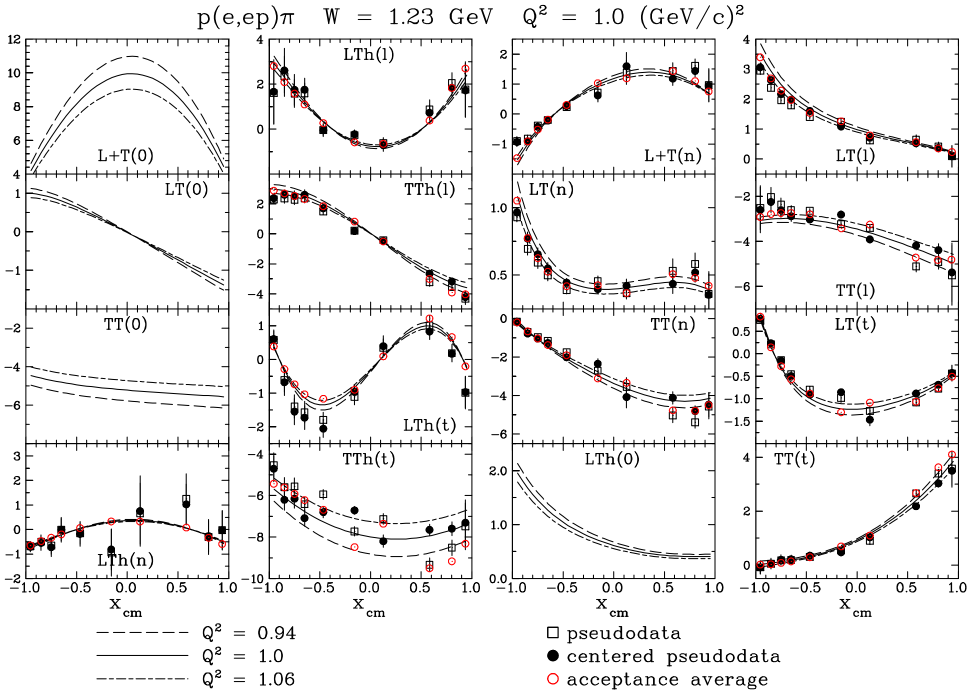

FIG. 2: Pseudodata data for response functions at $W = 1.23 \pm 0.01$ GeV and $Q^2 = 1.0 \pm 0.2$ (GeV/c)^2 are compared with the input model (MAID2000) at the central kinematics and neighboring values of Q^2 representative of the x dependence of acceptance averaging. Acceptance-averaged calculations are shown as red open circles and pseudodata as open squares. Filled circles show pseudodata with multiplicative kinematical corrections based upon the dipole form factor.

multiplicative procedure does not compensate for variations of $\overline{W}$, but the variations in $\overline{W}$ are much smaller than those in $\overline{Q^2}$. Figure 2 compares pseudodata with multiplicative kinematical corrections with the model for central kinematics. We again find that the corrections move the pseudodata in the directions indicated by ratios between acceptance averaged calculations and those for central kinematics. The net effect is to reduce the scatter in the pseudodata and to remove many systematic deviations attributable to the x dependence of $\overline{Q^2}$. On the other hand, we have the qualitative impression that the corrections are sometimes a little too large, although no attempt has been made to quantify that impression. One could reduce the size of the multiplicative correction by increasing Λ, but the $N \to \Delta$ form factor is actually steeper (smaller Λ) than the standard dipole form factor. Furthermore, changes to the correction by replacing the dipole with a parameterization of the $N \to \Delta$ form factor are quite small. Therefore, we will adopt the multiplicative correction based upon the dipole form factor as the standard method for bin centering.

B. Sensitivity of polarization to $\phi - \overline{\phi}$

Next we consider the sensitivity of polarization to acceptance averaging. Figures 3 and 4 show acceptance averaged calculations, using MAID2000, of polarization for $W = 1.23 \pm 0.01$ GeV and $Q^2 = 1.0 \pm 0.2$ (GeV/c)^2. The averages were accumulated at the target in the cm frame before spin transport and do not require any FPP analysis. Also shown are direct calculations for $W = 1.23$ GeV and $Q^2 = 0.9$, 1.0, and 1.1 (GeV/c)^2 but the three curves are practically indistinguishable. Evidently the variation of response functions with Q^2 tends to divide out, supporting the accuracy of the multiplicative method of bin centering. Acceptance averaging of ϕ is important for the helicity-independent polarizations and the best agreement with the input model is obtained by plotting data at $\overline{\phi}$ instead of ϕ. The situation for helicity-dependent polarization is less clear. The dip in P_t' for $\phi \sim 180°$ appears to be described better using ϕ than $\overline{\phi}$, but there appears to be slight reduction in overall strength also. Maybe the scale error is sensitive to acceptance averaging of ν_{LT}' and ν_{TT}', which are small and rather sensitive to ϵ when $\epsilon \to 1$ for the present beam energy. Nevertheless, our overall impression is that polarization data should be analyzed using $\overline{\phi}$.

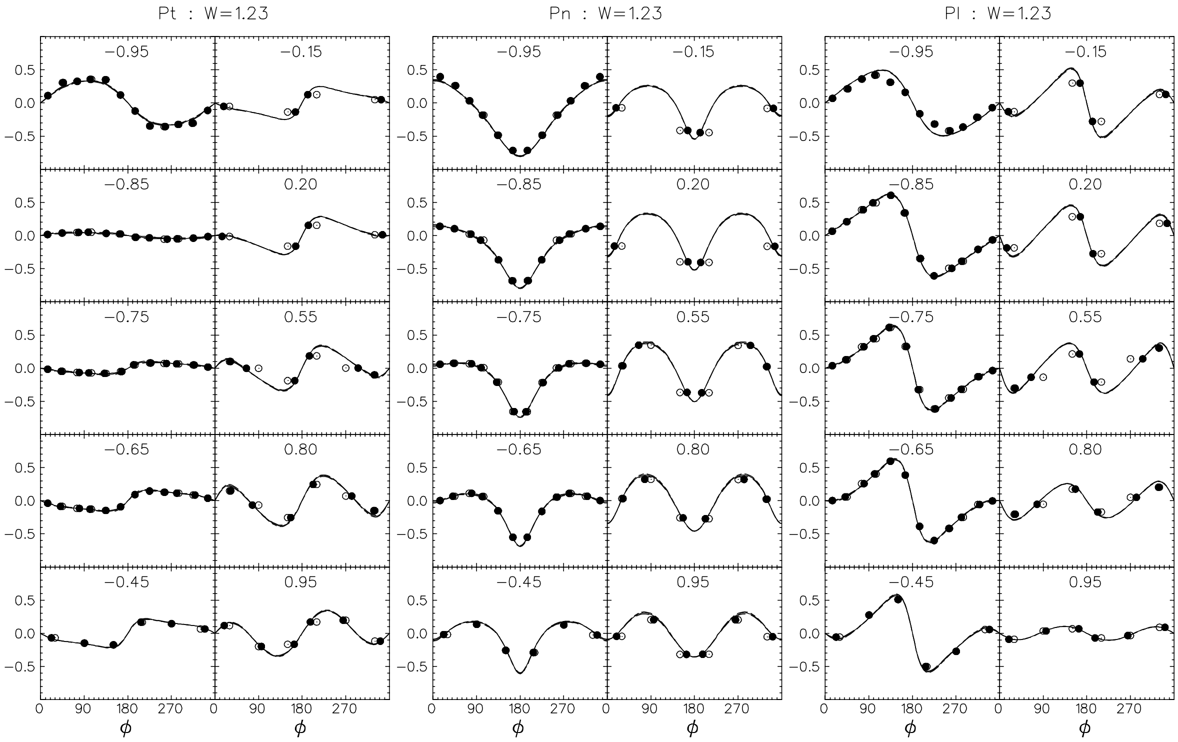

FIG. 3: Acceptance averaing of helicity-independent polarization for $W = 1.23 \pm 0.01$ GeV and $Q^2 = 1.0 \pm 0.2$ (GeV/c)^2 using MAID2000. Open circles are plotted at nominal values while filled circles are plotted at averaged values of ϕ. MAID2000 curves are plotted for $Q^2 = 0.9$, 1.0, and 1.1 (GeV/c)^2 but are practically indistinguishable.

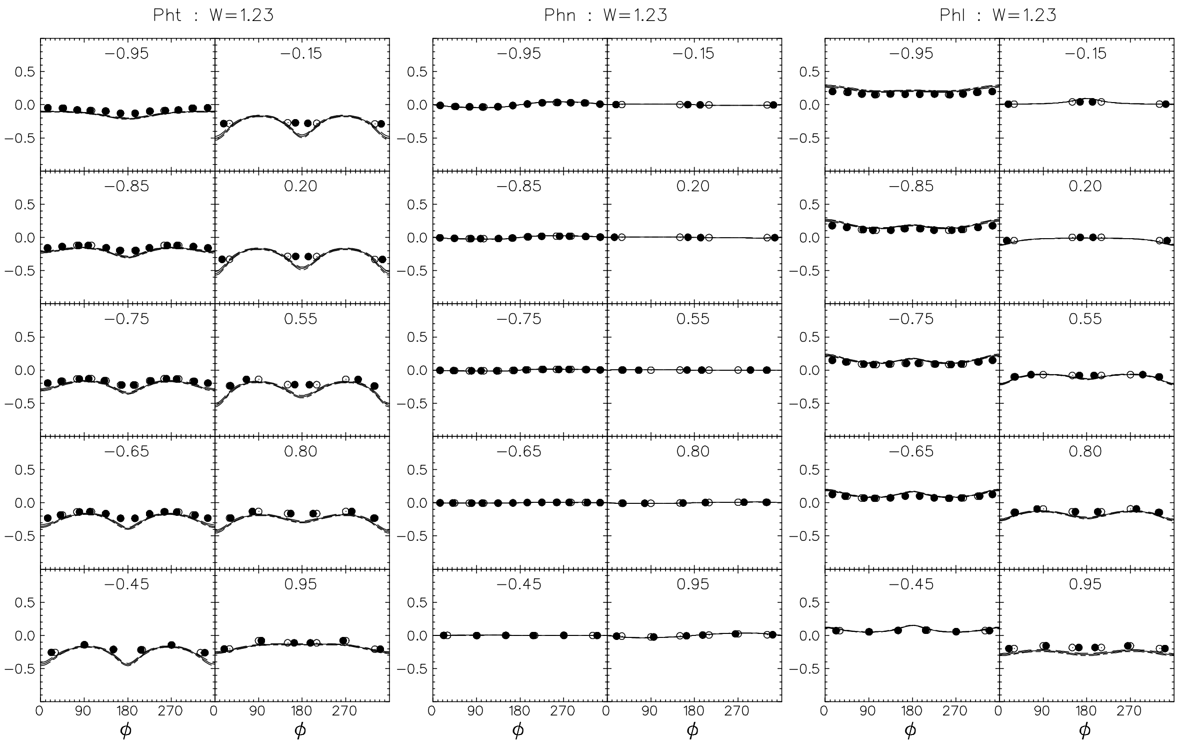

FIG. 4: Acceptance averaing of helicity-independent polarization for $W = 1.23 \pm 0.01$ GeV and $Q^2 = 1.0 \pm 0.2$ (GeV/c)^2 using MAID2000. See Fig. 3 for legend.

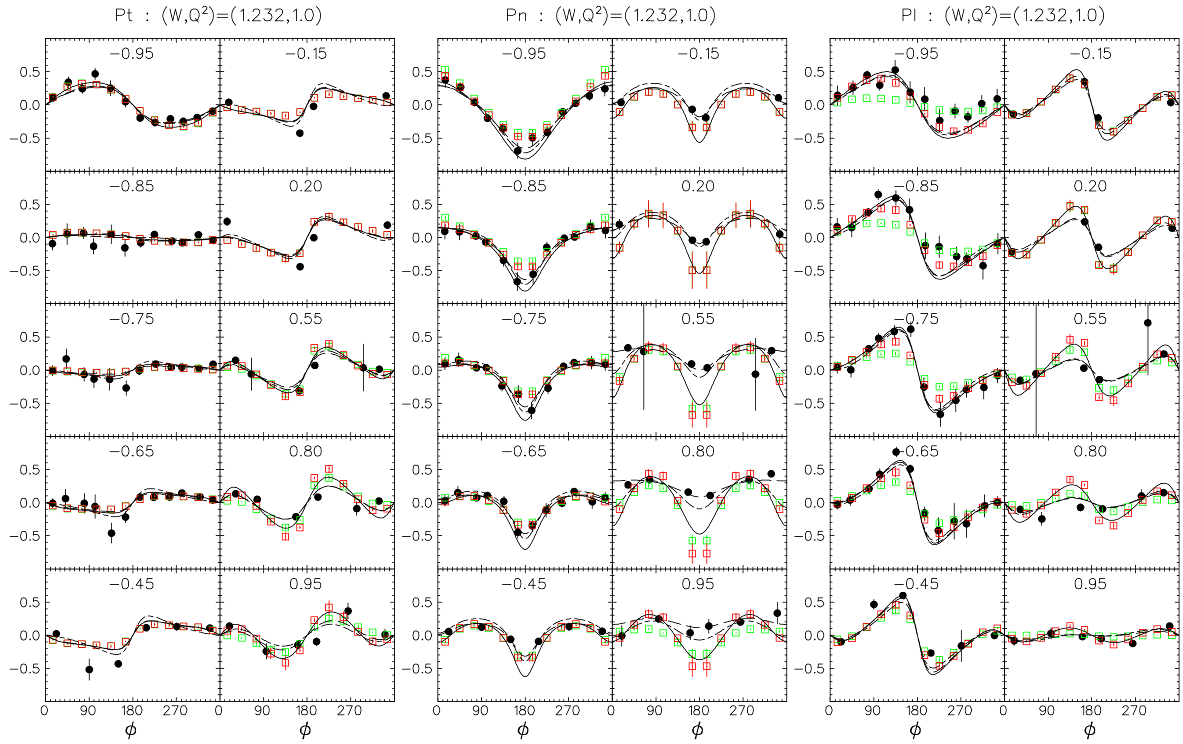

FIG. 5: Analysis of helicity-independent polarization from PALM pseudodata for $W = 1.232 \pm 0.02$ GeV and $Q^2 = 1.0 \pm 0.2$ $(\mathrm{GeV}/c)^2$. Black filled circles: polarization data from `PALM`. Green open squares: computed using MAID2000 cross sections and `PALM` data for response functions. Red open squares: computed from `PALM` data for reduced response functions. Solid lines: MAID2000. Dashed lines: Legendre fits to polarization data (black circles). Dash-dotted lines: multipole fits to polarization data.

III. CONSISTENCY BETWEEN POLARIZATION AND RESPONSE FUNCTIONS

Figures 5 and 6 evaluate the polarization pseudodata. The black circles are the polarization data directly from the PALM analysis, plotted at $\overline{\phi}$. The squares are polarizations computed from the response functions obtained from PALM where green is used for unreduced and red for reduced response functions. These were produced on a uniform grid of ϕ and propagate uncertainties in response functions. The cross section was calculated using the MAID2000 because the PALM pseudodata used that model for the cross section in its analysis of response functions; error propagation for these calculations do not include uncertainties in cross section. There appears to be a definite preference for using reduced response functions to calculate polarization, especially when $|x| \to 1$ gives the most rapid variation for the angular weight of some of the response functions. This effect is particularly pronounced in P_ℓ for parallel and P_n for antiparallel kinematics but is generally small in the middle of the x distribution. Therefore, the most accurate analysis applies all known angular factors event by event to minimize the effects of acceptance averaging. Consequently, the final data will be reported in terms of reduced response functions instead of polarizations.

The solid curves show calculations for the input model, MAID2000, at central kinematics. Polarizations computed from PALM pseudodata for response functions are usually quite close to the input model, but PALM polarizations are sometimes substantially different from the input model. Furthermore, most of the nonstatistical deviations are similar to discrepancies previous observed in the real data. For example, the PALM pseudodata for P_ℓ at $x = -0.95$ violate the expected geometrical symmetry with respect to $\phi = \pi$, with pseudodata for large ϕ being systematically suppressed relative to both the input model and the pseudodata for reflection across the scattering plane. Similarly, P_n pseudodata for $x > 0.2$ show surprisingly large positive values for at both ends of the ϕ distribution (the *bedposts* problem) and miss the strong negative dip for $\phi \sim \pi$ predicted by the input model. Both of these problems were present in the real data; in fact, these problems and the symmetry violation in P_ℓ provided much of the original motivation for rewriting `PALM` in C++ and performing this pseudodata analysis. It appears that these problems are caused neither by an unknown instrumental failure nor by bugs in the analysis program, but are primarily due to averaging over relatively coarse ϕ bins when some of the spin-transport coefficients have large kinematical variations. This hypothesis is discussed at more length below. The binning in ϕ was designed to achieve a fairly uniform level of statistical precision even for $x > 0$ where the acceptance shrinks and background grows.

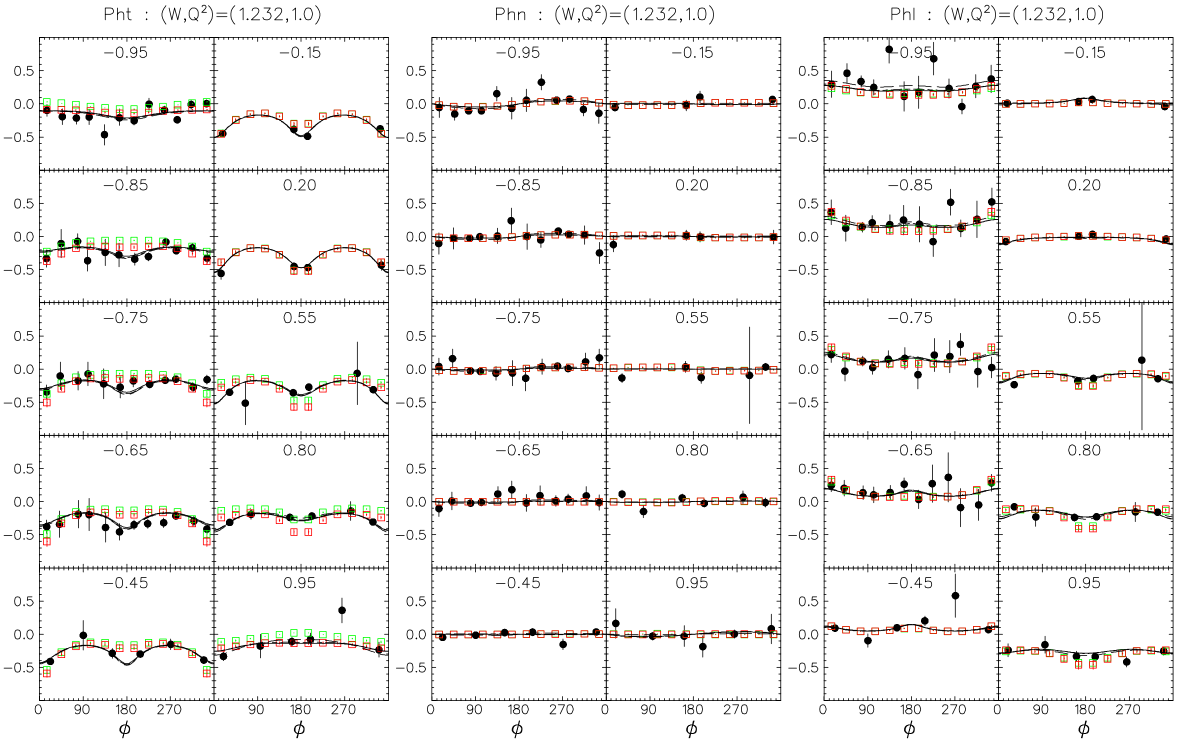

FIG. 6: Analysis of helicity-dependent polarization from PALM pseudodata for $W = 1.232 \pm 0.02$ GeV and $Q^2 = 1.0 \pm 0.2$ $(\mathrm{GeV}/c)^2$. See Fig. 5 for legend.

Figures 5 and 6 also show fits to the polarization pseudodata using Legendre coefficients (dashed curves) or multipole amplitudes (dashed-dotted curves). Both models describe the polarization pseudodata better than the input model but neither can reproduce the symmetry violation of P_ℓ because geometrical symmetries are built into both models. The Legendre analysis can handle the P_n pseudodata for $\phi \sim \pi$ best. However, the differences between the fits and the input model show that there are important systematic errors in the polarization pseudodata.

Figure 7 evaluates the results for response functions. We use reduced response functions unless specifically noted otherwise. For polarized response functions the black points show the PALM results directly. Therefore, the response pseudodata agree well with the input model, shown by red curves. Legendre fits to the response pseudodata (black points) are shown by black dashed curves and are generally quite close to the input model; most deviations can be ascribed to statistical fluctuations of the pseudodata instead of systematic distortion. The largest differences between fitted and input response are seen in R^{ℓ}_{TT} and R'^{t}_{TT} but are fairly similar to the uncertainties in the fitted responses.

Figure 7 also shows as green points response functions fit to the ϕ dependence of the PALM polarization pseudodata. Because response functions depend upon x, this method of extraction cannot accommodate variations of x with respect to ϕ. Therefore, the green points are shown at nominal x values while the black points are shown at acceptance-averaged values. Although some of the shifts are not negligible, those shifts alone cannot explain the strong differences seen in some of the response functions. Note that the black points include multiplicative corrections for variations of $\overline{Q^2}$ with respect to x but the green points do not; however, because the differences are often much larger than the bin-centering corrections shown in Fig. 2, this effect does not explain the differences between green and black data sets either. The green dash-dotted curves show response functions calculated from Legendre coefficients fit to the polarization pseudodata. The reasonable agreement between green curves and green points suggests that the discrepancy between the two pseudodata sets is not caused by problems in analyzing the ϕ dependence but reflects a basic inconsistency between the polarization and response pseudodata. The good agreement between the black points and the red curves shows that pseudodata for response functions are much more reliable than those for polarizations.

The systematic errors in the PALM data for P_ℓ for $x > 0$ produce large errors in the R^{ℓ}_{TT} fit to those data. The symmetry violation for P_ℓ at $x = -0.95$ appears in R^{ℓ}_{TT} as an anomalous point. It is important to recognize that errors in R^{ℓ}_{TT} and R^{ℓ}_{LT} are correlated because they are derived from the same polarization component; the effects appear larger for R^{ℓ}_{TT} because its the kinematic coefficient for its contribution to P_ℓ is generally smaller. Significant errors are observed in several other response functions for similar reasons, with corresponding correlations between quantities derived from a common polarization component. Unfortunately, the `EPIPROD` algorithms for

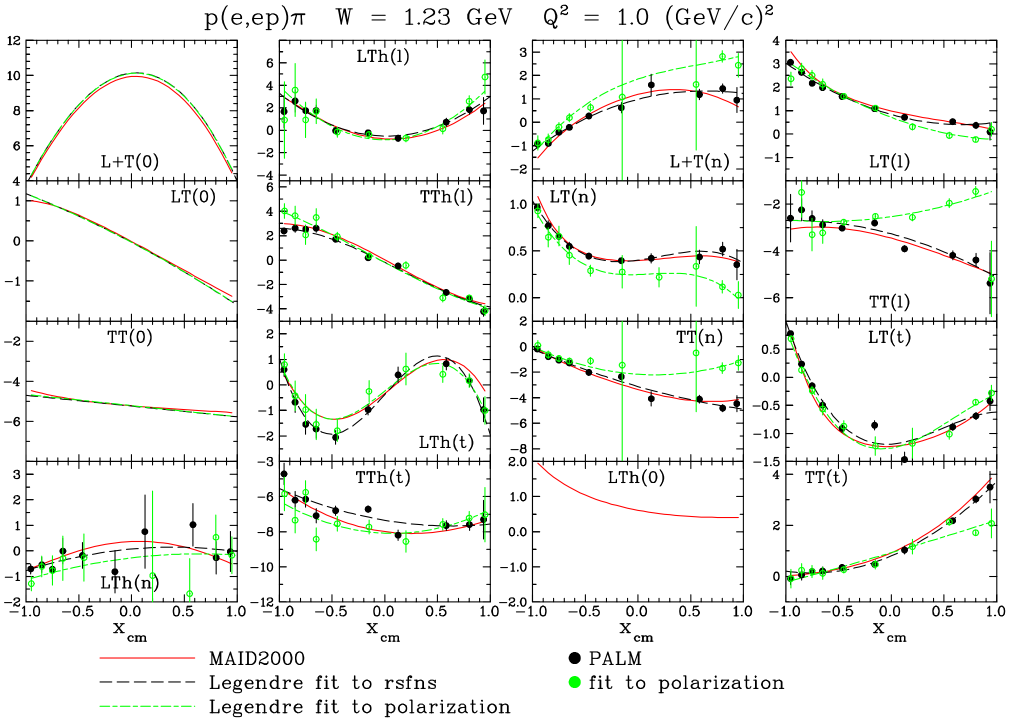

FIG. 7: Legendre fits to PALM pseudodata for $W = 1.232 \pm 0.02$ GeV and $Q^2 = 1.0 \pm 0.2$ $(\mathrm{GeV}/c)^2$. Black points: response function data from `PALM`. Green points: response functions extracted from the ϕ dependence of polarization data. Red solid lines: MAID2000. Dashed curves: fits to data for response functions. Dash-dotted curves: fits to data for polarizations. Note that cross section data were replaced by MAID2000 calculations with experimental error bars.

fitting Legendre coefficients or multipole amplitudes consider data points to be independent and are ignorant of such correlations. Although the black points are also correlated, these effects are probably much smaller when the response functions are obtained directly than when they are extracted from the ϕ dependence of binned polarizations.

Figure 8 shows a multipole analysis of the same data. Multipole fits to the response data are consistent within uncertainties with the model input. The failures of the multipole analysis of polarization are similar to those of the Legendre analysis. Therefore, the final analysis for real data should emphasize reduced response functions, using multiplicative bin centering, and should not use binned polarization data.

IV. DISCUSSION

The bottom line is that the PALM analysis for response functions appears to be internally consistent but that the method fails for the polarization. Although the polarization analysis appears to be reasonably accurate for some kinematics, the systematic errors for other kinematics and the violation of symmetries are sufficiently severe that one cannot extract responses or multipole amplitudes from the polarization directly with sufficient accuracy. The main difference between the two analyses is the explicit handling of the ϕ dependence in the response analysis, which avoids binning with respect to ϕ. It appears that the polarization analysis encounters trouble when the relevant spin transport coefficients exhibit broad distributions in ϕ within a particular x bin. For example, Fig. 9 displays scatter plots for spin-transport matrices for $x = -0.95$ versus ϕ_{xq}. Most of the sensitivity to P_ℓ is provided through $S_{x,\ell}$, which is relatively small and has a rather broad distribution. Furthermore, unlike some of the other matrix elements, there is no obvious ϕ symmetry; in particular, it does not share the ϕ symmetry of the observable. This appears to be an unpromising situation for bin averaging, which depends upon factorization of the form $\langle S_{x,\ell} P_\ell \rangle \approx \langle S_{x,\ell} \rangle \langle P_\ell \rangle$, and may be responsible for the failure of P_ℓ for $x = -0.95$ to obey the geometrical symmetry with respect to ϕ. Unfavorable correlations between ϕ and other variables may also worsen this problem, but that is purely speculative at this point. A large part of $S_{x,\ell}$ is due to the cm to lab transformation because the momentum swings through a large angle. Although we do not have a complete set of figures, we have observed that artificial elimination of this transformation improves the symmetry of P_ℓ pseudodata for $x = -0.95$.

Similarly, Fig. 10 shows that most of the sensitivity to P_n for $x = 0.80$ is provided by $S_{x,n}$ which is also relatively

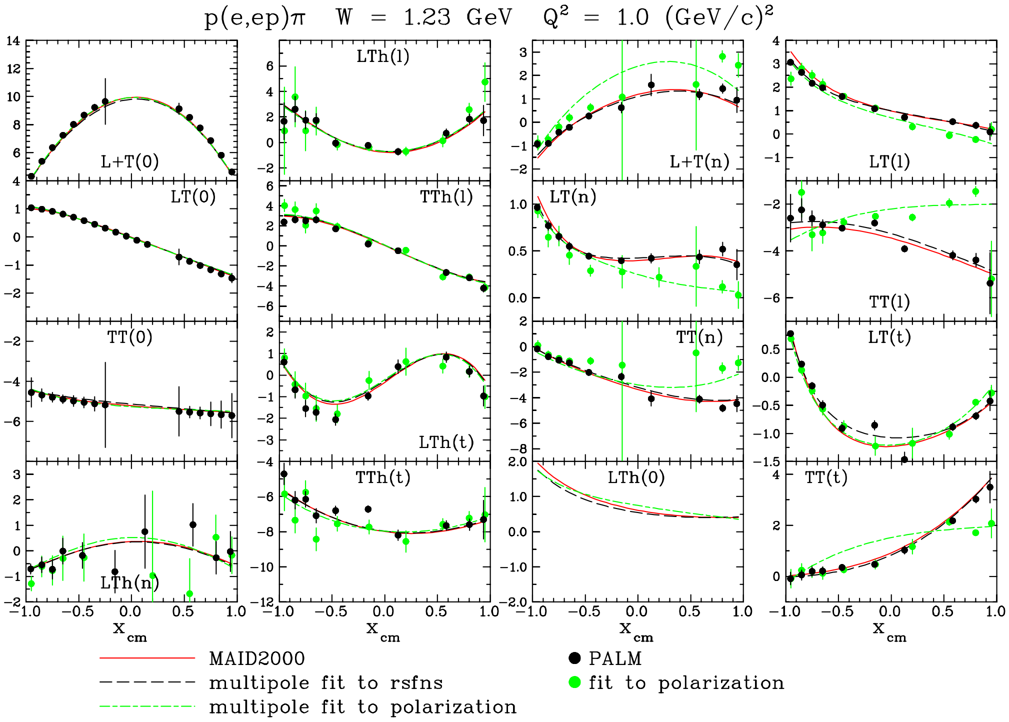

FIG. 8: Multipole fits to PALM pseudodata for $W = 1.232 \pm 0.02$ GeV and $Q^2 = 1.0 \pm 0.2$ (GeV/c)^2. Black points: response function data from PALM. See Fig. 7 for legend.

small and rather broad. Coincidentally, these undesirable properties generally occur where one of the matrix elements for longitudinal polarization at the focal plane becomes large. Although that component should be invisible to this experiment, the fact that it is large may contribute to the breakdown of factorization and the failure of polarizations binned in ϕ to reproduce model calculations for central kinematics.

Unfortunately, these qualitative arguments do not really prove that the width of the distributions for spin-transport coefficients is the primary difficulty for the polarization analysis. We have had other plausible hypotheses that did not explain the problem. One method for testing this argument might be to fit simple functions $S_{ij}(x,\phi)$ to these distributions and then to repeat the pseudodata analysis. If the extracted polarization pseudodata move closer to the model calculations but still show difficulties, one could arbitrarily flatten the ϕ dependencies of those functions to reduce further the effects of acceptance averaging at the focal plane. However, we do not have the time or manpower to conduct such studies at this late date. Such studies could help us to understand the problem, but would not necessarily provide much guidance for improving the analysis of polarization. Removing the ϕ dependence from the reconstructed quantities, in other words the response-function analysis, is probably very close to the optimal solution to this problem anyway. Therefore, the best strategy is to abandon the polarization analysis and concentrate upon finishing the analysis of response functions as quickly as possible. Further exploration of the polarization problem might be an interesting academic exercise, and maybe fodder for a possible NIM paper upon our extension of the likelihood method to recoil polarization, but is not our highest priority.

V. CONCLUSIONS

We have performed a pseudodata test of maximum-likelihood algorithms for analysis of recoil polarization angular distributions for pion electroproduction near the Δ resonance using the JLab Hall A spectrometers and focal-plane polarimeter. We find that pseudodata for response functions are faithful to the input model provided that suitable procedures are employed to compensate for acceptance averaging. The most important effect is the variation of $\overline{Q^2}$ with x and can be described by scaling according to the standard dipole form factor. Fits of Legendre coefficients or multipole amplitudes should also employ acceptance-averaged $\overline{x}$. Finally, the most reliable results are obtained using reduced response functions for which the leading powers of $\sin\theta_{cm}$ are explicitly included in the likelihood function. Eventwise handling of kinematic and geometrical variables minimizes the effects of acceptance averaging and we obtain results for response functions, Legendre coefficients, and multipole amplitudes that consistent with the input model.

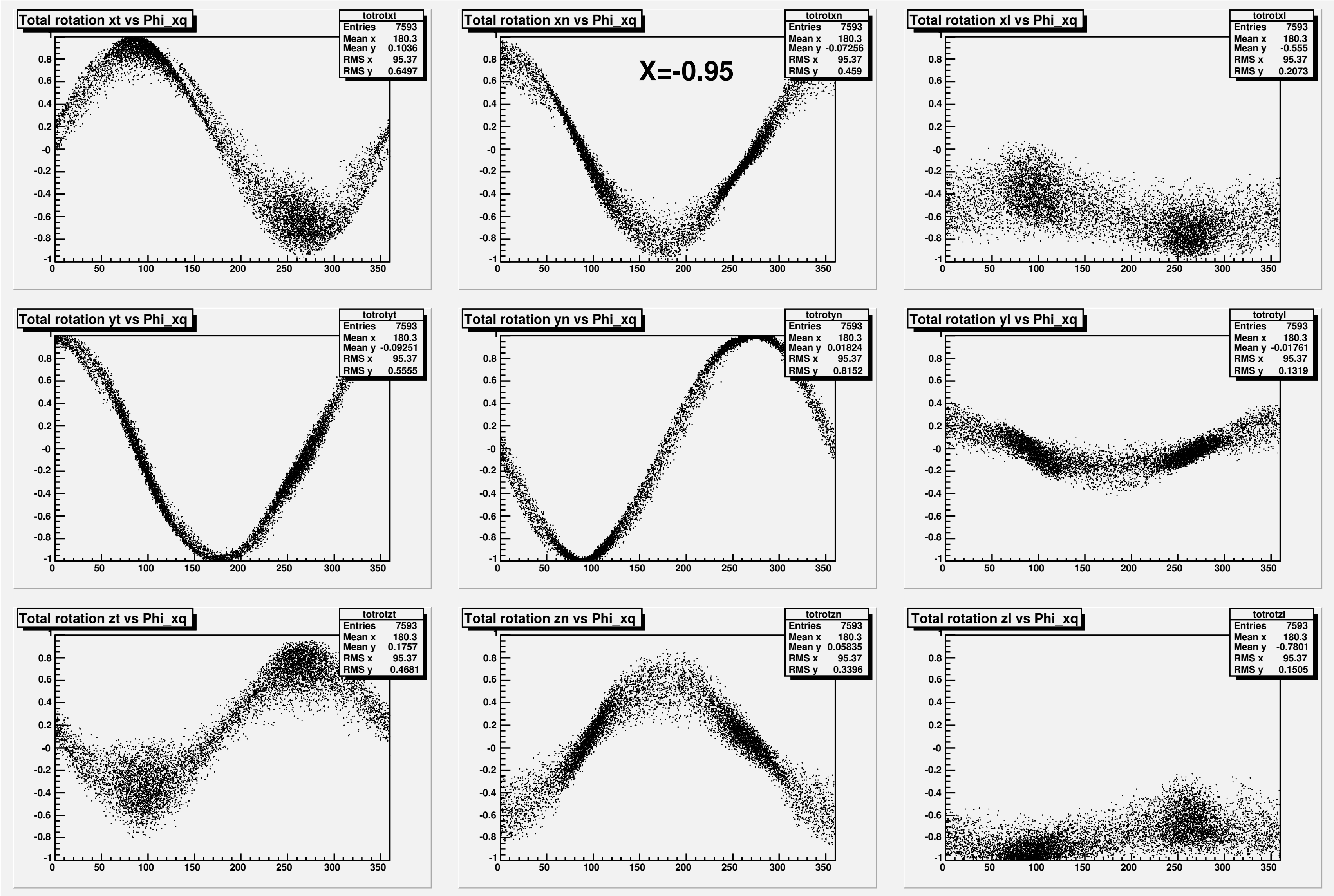

FIG. 9: Scatter plots for spin matrix elements at $x = -0.95$.

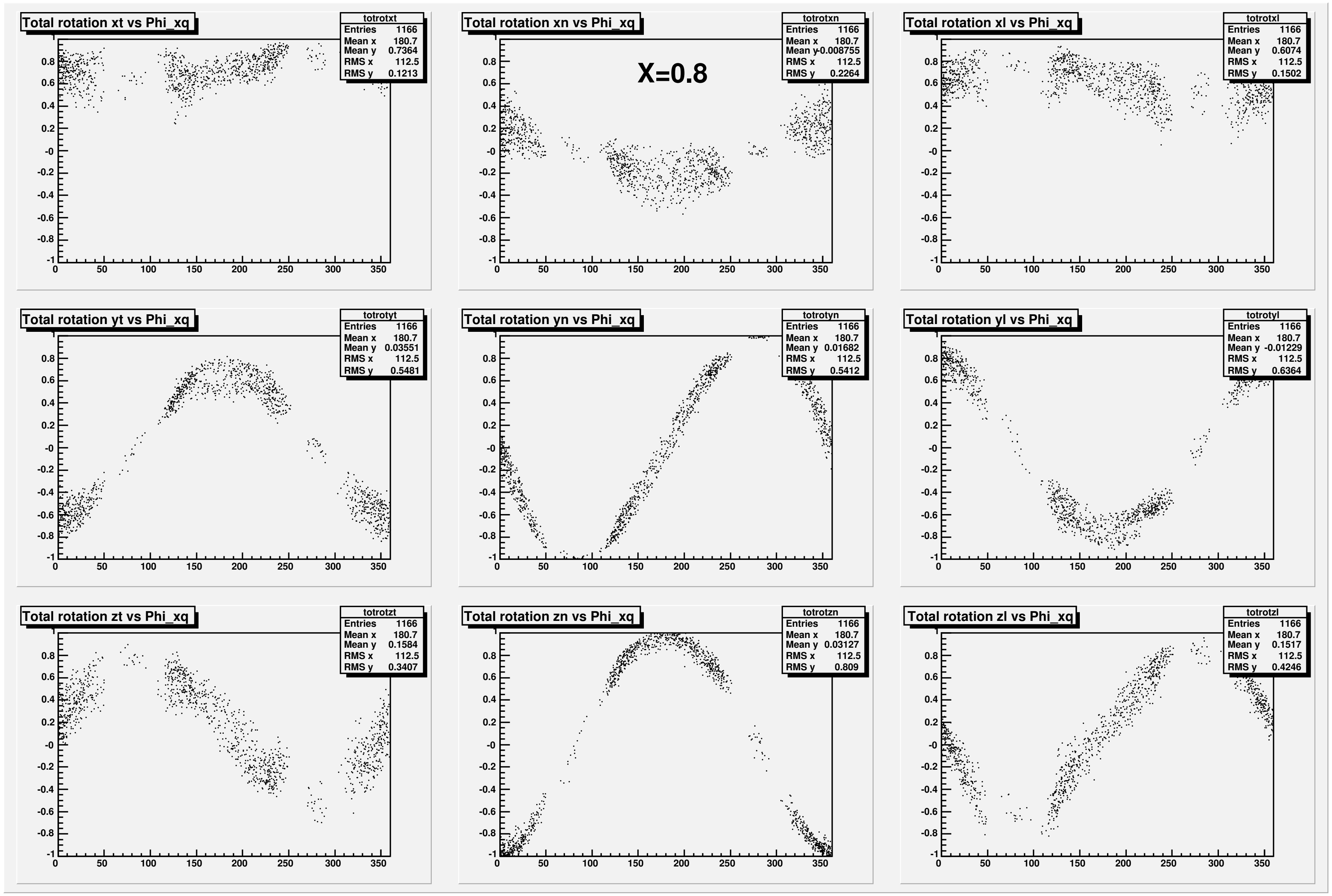

FIG. 10: Scatter plots for spin matrix elements at $x = 0.8$.

The extraction of polarization data binned with respect to (W, Q^2, x, ϕ) is much more problematical and we sometimes see substantial discrepancies between polarization pseudodata and acceptance-averaged model input. Some of the polarization pseudodata violate basic geometrical symmetries or display other implausible features. Response functions fit to the ϕ dependence of polarization pseudodata sometimes disagree strongly with response pseudodata extracted directly using eventwise kinematic and geometric factors. These systematic errors seriously distort Legendre or multipole fits to polarization pseudodata and there appears to be no way to recover reliable responses or multipoles from polarization data binned in ϕ, at least for the conditions and binning scheme for JLab experiment e91011.

Most polarization components include two or more response functions whose kinematical coefficients vary strongly within a 4-dimensional bin. Furthermore, some of the spin-transport coefficients exhibit broad kinematical distributions within a (W, Q^2, x, ϕ) bin. The kinematic focussing of the reaction into a cone with opening angle of about $\pm 13^\circ$ in the lab allows one to access all of the response functions, even though the spectrometers have relatively small acceptance and move in a plane, but the price is a factor of roughly 10 magnification of the measured polar angle upon transformation to the cm. Such magnification spoils the factorization of reaction kinematics, spin transport, and response functions needed to compare polarizations binned in ϕ to response functions for acceptance-averaged kinematics. The R^ℓ_{TT} response function is most sensitive to factorization errors because its contribution to P_ℓ is proportional to $\sin^2\theta \sin 2\phi$ and depends strongly upon the out-of-plane acceptance; furthermore, the $S_{x,\ell}$ spin-transport coefficient has a broad distribution that does not share the symmetry of P_ℓ. Systematic errors in R^ℓ_{TT} also affect R^ℓ_{LT} because response functions derived from a common polarization component tend to be highly correlated.

Therefore, the final analysis for this experiment will be based upon reduced response functions and will employ multiplicative bin centering. The polarization data will be extracted, partly because it is free and partly because colleagues still ask to see them, but will not be presented in publications. The data for reduced response functions and the corrections for small residual acceptance averaging effects are reliable and we can perform the multipole analysis with confidence.